BASE STATION POLARIZATION-SENSITIVE ADAPTIVE ANTENNA FOR MOBILE RADIO

Ioannis Kaptsis and Keith G. Balmain

Electromagnetics Group, Department of Electrical and Computer Engineering
University of Toronto
10 King's College Road, Toronto, Ontario M5S 1A4, Canada

ABSTRACT An attractive alternative to combat desired-signal fading and suppress co-channel interference in a mobile radio environment is to use a base station adaptive antenna with polarization-sensitive elements. This paper describes the design of a four-crossed-dipole adaptive array in which polarization discrimination is used to separate the desired signal from both directional and non-directional wave interference. In contrast to previous work, mutual coupling has been included in the evaluation of the array performance, using the method of moments. Further, computer simulation shows that the performance of the adaptive antenna is improved in the presence of a flat-backed corner reflector.

1. Introduction

In a wireless environment, a signal conveyed through a narrow-band channel becomes impaired mainly by Rayleigh-like fading and cochannel interference. The Rayleigh-like fading is caused by the multipath propagation of the desired signal while co-channel interference is introduced by the multiple use of the same frequency band. The simplest technique to maintain acceptable interference levels and at the same time keep up with the rapid increase of subscribers employs the use of antenna diversity at the base site. Adaptive antenna arrays also have the ability to reduce the effects of multipath fading and suppress interfering signals.

In this paper an adaptive base station antenna combined with a polarization diversity scheme is considered. An adaptive antenna with elements able to respond to more than one polarization can automatically track the desired signal with one polarization and null interference with a different polarization. In spite of the extensive literature in adaptive arrays, most studies have ignored mutual coupling among radiating elements. However, it is well documented that mutual coupling can alter significantly both the steady state and the transient response of an adaptive antenna [1]. In this work mutual coupling is calculated using the method of moments. Furthermore, the influence of a flat-backed corner reflector on the performance of the adaptive antenna is investigated. Extensive computer simulations show that the signal-to-noise ratio of the adaptive antenna is improved when the reflector is present.

0-7803-1823-4/94 $4.00 © IEEE

2. Mutual coupling effects on adaptive arrays

In a mobile radio environment not only is the signal arrival direction unknown but also it varies while the user moves. The least mean square (LMS) algorithm is thought to be the most suitable one in our case because it can automatically track either the desired or the interfering signal. A polarization-sensitive LMS adaptive array using two pairs of crossed dipoles as radiating elements has been studied by Compton [2], whose analysis did not include mutual coupling between the antenna elements.

The most commonly accepted measure of the steady-state performance of an adaptive antenna is the output signal-to-interference-plus-noise ratio (SINR). In order to find an expression for the output SINR one must know the element output voltages. These voltages will be used as the input signals to the adaptive processor. Therefore, we will derive an expression for the element output voltages when mutual coupling is taken into account.

Suppose the desired signal is incident on the array from the direction θ_d, ϕ_d with polarization P_d. This signal produces a signal vector

$$\mathbf{X}_d = A_d e^{j(\omega_0 t + \Psi_d)} \mathbf{V}_d \tag{1}$$

In addition m interfering signals at the same frequency as the desired one arrive from directions θ_{ik}, ϕ_{ik} and polarizations P_{ik}, contributing a signal vector

$$\mathbf{X}_{ik} = A_{ik} e^{j(\omega_0 t + \Psi_{ik})} \mathbf{V}_{ik} \tag{2}$$

Finally assume that an uncorrelated, zero-mean thermal noise of power σ^2 is present in each element signal. The total input signal vector is

$$\mathbf{X} = \mathbf{X}_d + \sum_{k=1}^{m} \mathbf{X}_{ik} + \mathbf{X}_n \tag{3}$$

In eqs. (1) and (2), A_d and A_{ik} are the amplitudes of the desired and the kth interfering signals respectively, ω_0 is the carrier frequency, ψ_d is the carrier phase of the desired signal and ψ_{ik} is the carrier phase of the kth interfering signal at the coordinate origin. Finally $\mathbf{V}_d$ and $\mathbf{V}_{ik}$ are respectively the desired signal vector and the kth interfering signal vector defined as follows:

$$\mathbf{V}_d = \begin{bmatrix} f_1(\theta_d, \phi_d, P_d)\, e^{-j\phi_{d1}} \\ f_2(\theta_d, \phi_d, P_d)\, e^{-j\phi_{d2}} \\ \vdots \\ f_N(\theta_d, \phi_d, P_d)\, e^{-j\phi_{dN}} \end{bmatrix} \tag{4}$$

where $f_j(\theta,\phi,P)$ is the pattern response of the jth element to a signal incident from direction (θ,ϕ) with polarization P. ϕ_{dj} is the interelement phase shift between the jth element and the coordinate origin and N is the number of elements in the array. Also,

$$\mathbf{V}_{ik} = \begin{bmatrix} f_1(\theta_{ik}, \phi_{ik}, P_{ik})\, e^{-j\phi_{i1}} \\ f_2(\theta_{ik}, \phi_{ik}, P_{ik})\, e^{-j\phi_{i2}} \\ \vdots \\ f_N(\theta_{ik}, \phi_{ik}, P_{ik})\, e^{-j\phi_{iN}} \end{bmatrix} \tag{5}$$

where the notation is analogous to that of the desired signal. The desired and the interfering signals are assumed to be continuous plane waves and zero-mean processes uncorrelated with each other.

When mutual coupling effects are taken into consideration the output current vector $\mathbf{I}$ of the array elements can be calculated numerically by the method of moments:

$$\mathbf{I} = \begin{bmatrix} I_1 \\ I_2 \\ . \\ . \\ I_M \end{bmatrix} = \begin{bmatrix} Z_{11} & Z_{12} & \cdots & Z_{1M} \\ Z_{21} & Z_{22} & \cdots & Z_{2M} \\ . & . & \cdots & . \\ . & . & \cdots & . \\ Z_{M1} & Z_{M2} & \cdots & Z_{MM} \end{bmatrix}^{-1} \begin{bmatrix} V_1 \\ V_2 \\ . \\ . \\ V_M \end{bmatrix} = \mathbf{Z}^{-1}\mathbf{V} \tag{6}$$

where $\mathbf{Z}$ is the generalized impedance matrix and $\mathbf{V}$ is the induced voltage vector. M is the number of expansion functions on the array elements. The mnth element of $\mathbf{Z}$ is

$$Z_{mn} = -\int_{\Delta l_m} W_m E^s_n dl - Z^l_{mn} \tag{7}$$

and the mth element of $\mathbf{V}$ is

$$V_m = \int_{\Delta l_m} W_m E^i dl \tag{8}$$

where Δl_m is the segment on which the nth expansion function is located. W_m is the mth weighting function, E^s_n is the scattered field from the nth current expansion function, and E^i is the incident field. The Z^l_{mn} in eq. (7) equals the lumped loading impedance when $m=n$, otherwise $Z^l_{mn} = 0$.

Once the current distribution on the array elements is known from eq. (6), the array input signal vector $\mathbf{U}$ and the output voltage of each element can be obtained. For an N-element array, $\mathbf{U}$ can be written as

$$\mathbf{U} = (U_1, U_2, \ldots, U_N)^T = (I_{s_1} Z^l_1, I_{s_2} Z^l_2, \ldots, I_{s_N} Z^l_N)^T \tag{9}$$

where I_{s_j} (j = 1, 2,..., N) is the output current of the jth element. The subscript s_j denotes the expansion function number on the output terminal. Z^l_j is the lumped loading impedance attached to the jth element and in this paper it is $Z^l_j = Z^{l\,*}_{mm}$. T denotes the transpose and $*$ the complex conjugate. The covariance matrix Φ is given by

$$\Phi = E[\mathbf{X}^* \mathbf{X}^T] = A_d^2 \mathbf{U}_d^* \mathbf{U}_d^T + \sum_{k=1}^{m} A_{ik}^2 \mathbf{U}_{ik}^* \mathbf{U}_{ik}^T + \sigma^2 \mathbf{I} \tag{10}$$

with $\mathbf{I}$ the identity matrix. In order for the LMS array to track the desired signal, the reference signal $\tilde{r}(t)$ must be correlated with the desired signal and uncorrelated with the interfering ones. We assume that

$$\tilde{r}(t) = A_r e^{j(\omega_0 t + \psi_d)} \tag{11}$$

The reference correlation vector is then

$$\mathbf{S} = E[\mathbf{X}^* \tilde{r}(t)] = A_d A_r \mathbf{U}_d^* \tag{12}$$

and finally the output SINR of the array is given by

$$SINR = \xi_d \left(\mathbf{U}_d^T \mathbf{U}_d^* - \sum_{k=1}^{m} \frac{\left| \mathbf{U}_d^T \mathbf{E}_k^* \right|^2}{\| \mathbf{E}_k \|^2} \right) \tag{13}$$

where

$$\mathbf{E}_k = \mathbf{U}_{ik} - \sum_{n=1}^{k-1} \frac{\mathbf{U}_{ik}^T \mathbf{E}_n^*}{\| \mathbf{E}_n \|^2} \mathbf{E}_n \tag{14}$$

$\xi_d = \dfrac{A_d^2}{\sigma^2}$ is the input desired-signal-to-noise ratio (SNR) and $\xi_i = \dfrac{A_i^2}{\sigma^2}$ is the input interference-to-noise ratio (INR).

3. Dependence of adaptive antenna performance on conventional antenna design

It is often assumed that an adaptive antenna because of its flexibility can overcome most of the defi-

ciencies of the conventional antenna design. However, very serious problems such as grating nulls can arise with improper element positioning. Moreover, the output SINR of an adaptive antenna is related to the conventional array characteristics [3]. The output SINR degrades as an interfering signal approaches a sidelobe of the unperturbed pattern with the maximum degradation occurring when the interfering signal reaches the main beam. In contrast, the output SINR incurs no degradation at the nulls of the unperturbed pattern. Therefore it can be concluded that the narrower the main beam and the lower the sidelobes of the unperturbed pattern, the better the resolution of the adaptive array.

Taking these criteria into consideration we tried to optimize not only the geometry of the adaptive array itself but also the shape and the dimensions of the reflector. An array of four crossed dipoles spaced uniformly in (y,z) plane, as shown in Fig. 1, is the selected configuration. This configuration allows both the horizontal and the vertical receiving patterns of the antenna to be controlled by adjusting the phase and the amplitude of the radiating elements. Since the number of degrees of freedom of the adaptive processor has been increased, the antenna has the ability to null interfering signals over a wide range of incoming angles.

The length and the radius of the dipoles are l=0.471λ and r=0.001m respectively. They have been chosen so the imaginary part of the self impedance of each radiating element will be minimized. In order for good convergence to be obtained, each dipole has been divided into twelve segments (l=12d), so that a segment becomes as long as thirteen times the wire radius (d=13r), and less than 1/25 of the wavelength (d<λ/25).

A corner reflector structure alters significantly the conventional pattern of an antenna. The shape and the dimensions of the reflector are very important parameters in the pattern optimization process. It was found through extensive computer simulations using the multi-radius bridge current (MBC) thin-wire method-of-moments program [4] that a flat-backed corner reflector has better radiation performance than a conventional corner reflector. The reflector structure was simulated using a wire grid model. The distance between the wires of the grid model was d=0.125λ and the wire radius was calculated using the same-surface-area rule. Trying to optimize the radiation pattern of the antenna according to the aforementioned criteria and keeping the design as compact as possible, we arrived at the following dimensions. The length of the reflector is L=2λ, the width of the sides is W=1.5λ, the length of the planar section is R=2λ, and finally the distance of the crossed dipoles from the planar section and the interelement spacing are respectively S=0.6λ and D=0.8λ.

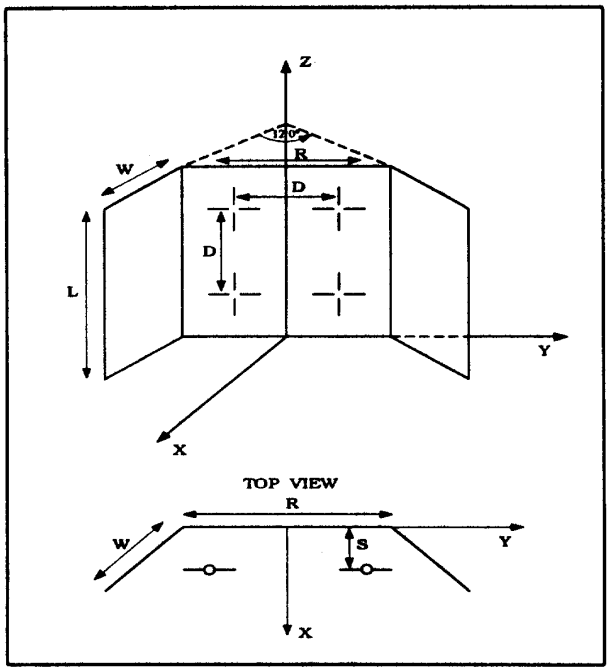

Figure 1. An array of four crossed dipoles in front of a flat-backed corner reflector.

The antenna operates over the 890-915 MHz band. When f=900 MHz the 3-dB beamwidth in the horizontal (x,y) plane is approximately 21° while the level of the sidelobes is -5 dB. In the vertical (x,z) plane the 3-dB beamwidth is 42° and the sidelobes are at least 10 dB lower than the main lobe.

4. Evaluation of the steady state performance of the adaptive antenna

We have already developed a formula for the signal-to-interference-plus-noise ratio of an LMS adaptive array, eq. (13), and now we can proceed with the evaluation of its performance. Figure 2 presents the output SINR as a function of the angle of incidence of the interfering signal, ϕ_i, when the flat-backed corner reflector is present and absent. In both cases the desired signal is a linearly polarized wave with polarization angle P_d = 45° and angle of incidence such that (ϕ_d, θ_d) = (0°, 90°) . The interfering signal has the same polarization state as the desired signal but its angle of incidence is varying. The input desired signal-to-noise ratio is 10 dB and the input interference-to-noise ratio is 30 dB. It can be observed that generally the output SINR is higher when the flat-backed corner reflector is present. When both signals arrive from the same direction, the output SINR drops significantly. This null is intrinsic to

the adaptive array and occurs simply because the array cannot distinguish between the desired and the interfering signals. Furthermore, the angular resolution of the antenna becomes higher when the reflector is present. This means that the separation between the angle of incidence of the desired and the interfering signal can be smaller without the output SINR dropping significantly.

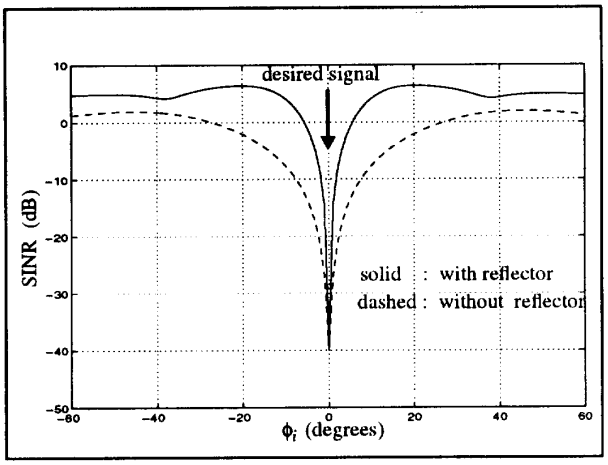

Figure 2. Output SINR performance versus ϕ_i.

Figure 2 presents the worst case since both signals come from the same direction and with the same polarization. In the following we will investigate how much difference in the polarization or the direction of arrival between the signals is required so the adaptive antenna can provide substantial protection.

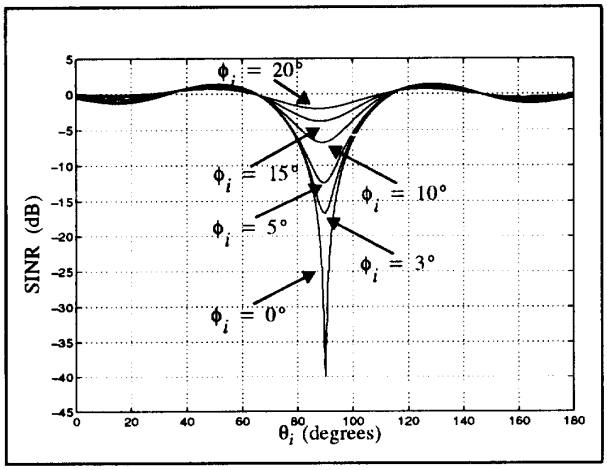

Figure 3. Output SINR performance of the antenna without the reflector, versus θ_i for different ϕ_i, $(\phi_d, \theta_d, P_d) = (0°, 90°, 45°)$.

Figure 3 shows the output SINR as a function of the direction of arrival of the interfering signal θ_i for different values of ϕ_i when the reflector is not present. The desired signal arrives from $(\phi_d, \theta_d) = (0°, 90°)$. Both the desired and the interfering signals have the same linear polarization $P_d = P_i = 45°$. In Fig. 4 the same family of curves is presented but with the reflector being present. In both cases the input SNR is 10 dB while the input INR is 30 dB. From Fig. 3 we can see that for $\phi_i = 20°$ and $\theta_d = \theta_i = 90°$ the SINR is almost -2 dB, which means that when ϕ_d is different from ϕ_i by only 20° the array can provide almost 38 dB protection against interference. When the reflector is present, Fig. 4 shows that only 5° difference is required to achieve the same SINR level.

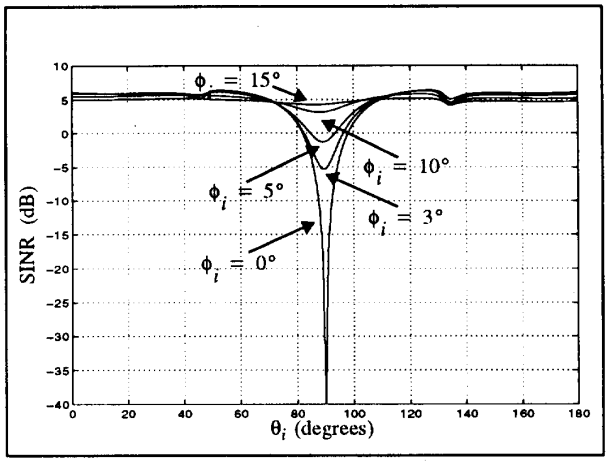

Figure 4. Output SINR performance of the antenna with the reflector, versus θ_i for different ϕ_i, $(\phi_d, \theta_d, P_d) = (0°, 90°, 45°)$.

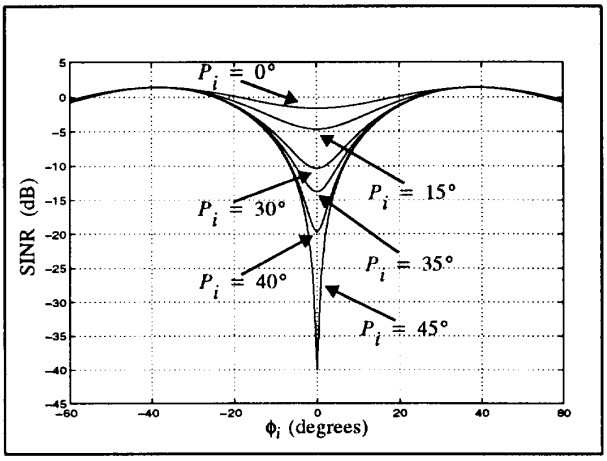

Figure 5. Output SINR performance of the antenna without the reflector, versus ϕ_i for different P_i, $(\phi_d, \theta_d, P_d) = (0°, 90°, 45°)$.

In all the above cases, it was assumed that the polarization of the desired signal is exactly the same as that of the interfering signal. It would be interesting to

evaluate the impact of the polarization of the incoming signals on the performance of the antenna. Figure 5 presents again the output SINR as a function of the polar angle ϕ_i, but this time for different angles of polarization of the interfering signal. The polarization and the angle of arrival of the desired signal remain the same. When the reflector is absent, a 15° difference between the polarization angle of the desired and the interfering signal is required for the antenna to provide 30 dB protection against interference. On the other hand, with the reflector present, the same amount of protection can be provided for a difference in the polarization angles of the incoming signals of less than 10°, as shown in Fig. 6.

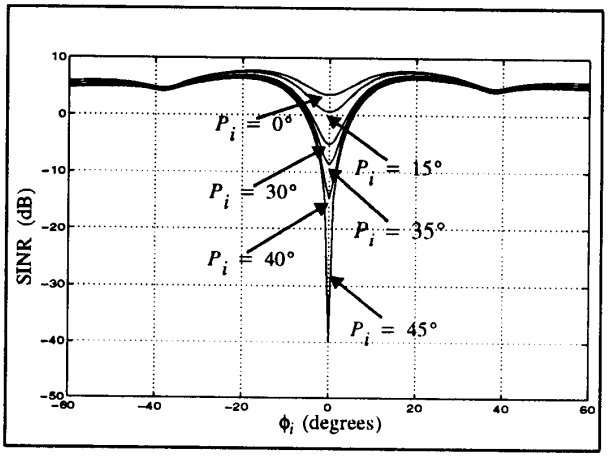

Figure 6. Output SINR performance of the antenna with the reflector, versus ϕ_i for different P_i; $(\phi_d, \theta_d, P_d) = (8°; 90°; 45°)$.

5. Adaptive antenna performance in the presence of multiple interfering signals

We have already evaluated the performance of the adaptive antenna with only one interfering signal being present. Let us now assume that we have more than one strong interfering signal. The presence of multiple interfering signals will cause higher degradation and this degradation will depend not only on the angular displacements of the interfering signals from the desired signal but also on the angles between the interfering signals. When the interfering signals are at large angular separations, the total degradation in the output SINR is the direct cumulative addition of the degradation due to each interfering signal. However, interfering signals with small angular separations will interact with each other [5].

Figure 7 shows the output SINR in the presence of one, two, and three interfering signals, with the reflector being absent. The desired signal is incident from $(\phi_d, \theta_d) = (0°, 90°)$. The first interfering signal is located at $(\phi_{i1}, \theta_{i1}) = (-35°, 90°)$, the second at $(\phi_{i2}, \theta_{i2}) = (20°, 90°)$ and the third one is swept across the whole range of the antenna in the horizontal plane.

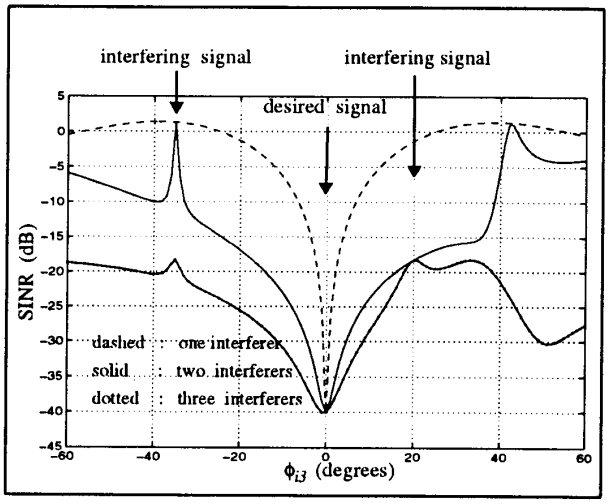

Figure 7. Output SINR of the antenna in the absence of the reflector with multiple interfering signals.

It is obvious that the output SINR degrades as the number of interfering signals increases. Physically, the SINR degradation may be explained in terms of the gain degradation of the radiation pattern of the array. When a single interfering signal is incident on the antenna, the adaptive processor adjusts the pattern so that a null is placed in the direction of the interfering signal. If it happens that the interfering signal appears at one of the existing nulls of the unperturbed pattern, there will be no change in the pattern and consequently in the SINR. Otherwise, the nulls of the array will be perturbed and the output SINR will be degraded. As a second interfering signal approaches the first one, the degradation in the output SINR starts increasing. The increased degradation is caused by the fact that now a second null has to be moved from its original position and thus the pattern, the gain, and finally the SINR will be degraded. The degradation will keep increasing until the two nulls coincide. When the incoming directions of the two interfering signals are exactly the same, a single null is adequate for handling both of them and the pattern reverts to the single interfering signal case.

The degradation in the adaptive array performance is related to the number of free nulls that are available. Their number is limited, so the distortion of the array pattern and finally the distortion of the output SINR will increase as the number of the interfering signals increases. Figure 8 presents the output SINR when the

flat-backed corner reflector is present for the same scenario as the one presented in Fig. 7. In this case average degradation of the SINR is much smaller compared with that when the reflector is absent.

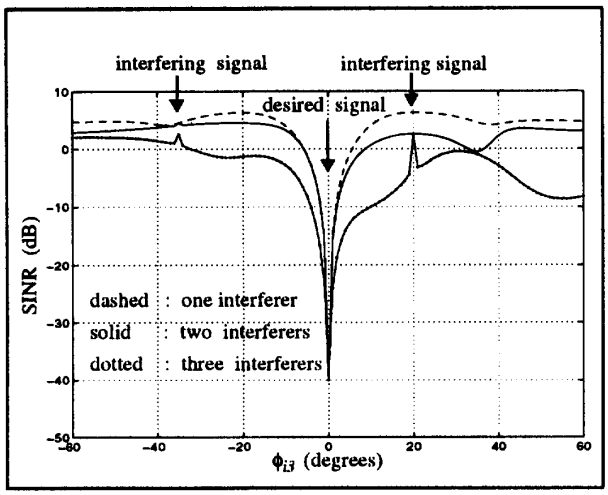

Figure 8. Output SINR of the antenna in the presence of the reflector with multiple interfering signals.

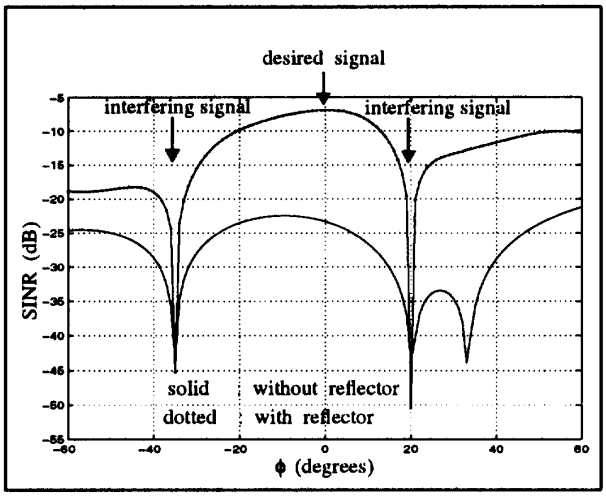

Figure 9. Adapted pattern of the antenna in the horizontal (x,y) pattern.

In order to demonstrate the improvement in the performance of the adaptive array when the reflector is present, we can plot the adapted pattern of the antenna both with and without the reflector. Figure 9 presents the adapted pattern of the antenna for the foregoing scenario. Comparing the two plots we can see that on average the received signal level is higher when the reflector is present. Moreover, in the absence of the reflector the main beam of the radiation pattern of the antenna is not pointing towards the exact direction of arrival of the desired signal. In contrast, when the reflector is present, the antenna not only can steer the main beam more accurately towards the direction of the desired signal but also can null interfering signals that are placed very close together.

6. Conclusions

The performance of a polarization-sensitive adaptive array of four crossed dipoles, intended to operate as a base station antenna in a land mobile environment, has been presented in this paper. The significance of the mutual coupling and the necessity for it to be considered as an important parameter in the design of the antenna ware pointed out. The steady-state response of the antenna has been evaluated both with and without the flat-backed corner reflector. Higher output SINR and better angular resolution can be achieved when the reflector is present. Finally, it was shown that polarization discrimination can be used to distinguish the desired from the interfering signals even if they arrive from the same direction.

7. Acknowledgment

The authors express their appreciation for the strong support and interaction provided by Bell Canada and Bell-Northern Research, and in particular by Mr. M.M. Cohen.

8. References

[1] I. J. Gupta and A. A. Ksienski, "Effect of mutual coupling on the performance of adaptive arrays," *IEEE Trans. Antennas Propagat.*, vol. AP-31, no. 5, pp. 785-791, 1983.

[2] R. T. Compton, Jr., "On the performance of a polarization-sensitive adaptive array," *IEEE Trans. Antennas Propagat.*, vol. AP-29, no. 5, pp. 718-725, 1981.

[3] I. J. Gupta and A. A. Ksienski, "Dependence of adaptive array performance on conventional array design," *IEEE Trans. Antennas Propagat.*, vol. AP-30, no. 7, pp. 549-553, 1982.

[4] M. A. Tilston and K. G. Balmain, "A multiradius, reciprocal implementation of the thin-wire moment method," *IEEE Trans. Antennas Propagat.*, vol. AP-38, no. 10, pp. 1636-1664, Oct. 1990.

[5] I. J. Gupta and A. A. Ksienski, "Prediction of adaptive array performance," *IEEE Trans. Aerospace Electron. Syst.*, vol. AES-19, no. 3, pp. 380-388, 1983.